# HIGH TEMPERATURE MECHANICAL PROPERTIES OF A $Si_3N_4$+SiC NANOCOMPOSITE

**J. Dusza**

***Abstract***

*Mechanical properties of a hot pressed silicon nitride/silicon carbide nanocomposite and the reference monolithic $Si_3N_4$ has been investigated at high temperatures in air using different mechanical tests; fracture toughness, dynamic fatigue, stepwise loaded low-cyclic fatigue and creep. Single-edge V-notched bend specimens were used for the fracture toughness test at different loading rates from 0.01 to 1.0 mm/min. The $K_{IC}$ value was calculated from the crack size prior to catastrophic fracture. The same loading rates were used for the dynamic fatigue test. Two types of specimens have been tested in stepwise loaded low-cyclic fatigue; without and with a sharp notch (notch tip radius ~10 $\mu$m) at loads from 50 N with steps of 50 N and with steps of 25 N, respectively. Five cycles have been made at each load with a loading amplitude of 50N up to the failure of the specimen. All these tests have been made at 1350°C. The creep test was performed in four-point bending mode in air in a temperature range from 1200°C to 1400°C. Fractography was used for the measurement of the size /shape of the slow crack growth (SCG) area and for the study of the fracture micromechanisms during the SCG propagation. The $Si_3N_4$+SiC nanocomposite exhibits better mechanical properties at high temperatures than the reference monolithic $Si_3N_4$.*

***Keywords: silicon nitride, silicon carbide, nanocomposite, microstructure, fracture toughness, strength, creep***

## INTRODUCTION

Silicon nitride based materials are one of the most promising candidates for structural application around the temperature of 1350°C. The utilization of $Si_3N_4$ ceramics as components in gas turbine and advanced automotive engines has received considerable attention over the last years with the main goal to optimize their fracture toughness, strength, creep and oxidation resistance. Using microstructural design (self-reinforcement by large elongated grains and tailoring the chemistry of the intergranular phase) a room temperature fracture resistance of more than 10 $MPam^{0.5}$ and fracture strength higher than 1 GPa have been achieved [1, 2]. As regards the high-temperature properties, these are controlled mainly by sintering aids, as MgO, $Al_2O_3$ + $Y_2O_3$ or $Y_2O_3$ and $Yb_2O_3$. Yttria and ytterbia have been found most refractory at high temperatures and are preferred for applications such as advanced gas turbine engines [3].

The type of fracture in $Si_3N_4$ ceramics at high temperatures depends mainly on the applied stress and on the environment. Slow crack growth or subcritical crack growth (SCG) and creep rupture are the typical failure mechanisms in these materials at elevated temperatures. SCG generally occurs by the extension of pre-existing flaws at relatively low temperatures and high stresses, and it is generally the result of an environmentally assisted

Ján Dusza, Institute of Materials Research, SAS, Košice, Slovak Republic

process. During creep the rupture failure is usually associated with bulk deformation (higher temperatures) and extensive nucleation, growth, and coalescence of cavities and microcracks as a result of diffusion, viscous flow, etc. Localized creep damage in the vicinity of the crack tip may occur in the SCG regime under certain conditions.

In spite of the intensive study of the high temperature fracture behaviour of $Si_3N_4$ ceramics during the last two decades, there are still some uncertainties mainly as regards the role of oxidation in the fracture process [4].

Damage regions initiating at the surface of specimens during high temperature tests were reported in silicon nitride ceramics by many authors, suggesting that oxidation is associated with their formation [5, 6]. Wereszczak et al. [7] defined these regions as stress-oxidation damage zones, which include the sum of all effects resulting from stress and oxidation. To examine if and how the oxidation affects the evolution of SCG and creep damage, flexure dynamic fatigue tests have been conducted in air and inert environment at 1370°C on $Si_3N_4$+ 6wt% $Y_2O_3$ samples. The strength exhibited stress rate independence in argon and nitrogen and no stress-oxidation damage zone was observed for any of the specimens tested under these environments. On the other hand, the strength significantly decreased with decreasing the stress rate in air and a stress-oxidation zone had formed in all tested specimens.

Wereszczak et al. [8] studied the evolution of stress-corrosion cracking (SCC) in PY6 silicon nitride ceramics at 1370°C during tensile creep rupture in air. Stress-corrosion cracking was observed as a surface-associated phenomenon consisting of mass removal (cations diffuse to the surface from the bulk and oxygen diffuses inwards) via evolution of two-grain and multigrain junctions within the near-surface volume, which was enhanced under tensile stress.

During the last years, $Si_3N_4$ + SiC nanocomposites were developed in which nano-sized SiC particles are dispersed in the $Si_3N_4$ matrix [9-11]. These particles are usually located either intragranularly, with a size of approximately 30 nm, or intergranularly, with a size of approximately 150 nm [11].

Three main methods have been used for processing such a nanocomposite: hot pressing (HP) or gas pressure sintering (GPS) of a mechanical mixture of crystalline $Si_3N_4$ and SiC powders of sub-micrometer size, HP of a CVD SiCN amorphous powder, and the combination of these methods: HP or GPS of a mixture of a crystalline $Si_3N_4$ + amorphous SiCN powders. During the last five years the high temperature mechanical properties of $Si_3N_4$ + SiC nanocomposites have been studied by a number of authors [12-14]. It was shown that these ceramics exhibit higher strength and better creep resistance than monolithic $Si_3N_4$. According to Rendtel et al. [15], strength of the $Si_3N_4$ + SiC nanocomposite at 1400°C lies between 80% and 100% of the room temperature strength, with creep rates as low as $1x10^{-9}$ $s^{-1}$ at 300 MPa and 1400°C. This behaviour can be explained by a thinner and more refractory intergranular phase of the composite compared to the monolithic material. This is caused by trapping of a significant amount of glass between SiC particles and by the presence of carbon in the intergranular phase [16]. Rouxel et al. [17] reported rising R – curves in a $Si_3N_4$ + SiC nanocomposite with a two fold increase in crack growth resistance after 1 mm crack extension. This was explained by time dependent visco-elastic mechanisms which result in rate dependent fracture characteristics. Recently excellent oxidation resistance was reported for $Si_3N_4$ + SiC nanocomposites compared to monolithic silicon nitride. This was mainly connected with the change in the oxidation and damage mechanisms during operation at high temperatures [18].

The aim of the present contribution is to study the influence of the addition of SiC nano-particles on the high temperature mechanical properties of silicon nitride.

## EXPERIMENTAL MATERIAL AND METHODS

The $Si_3N_4$ + SiC nanocomposite was prepared by using 20% of silicon carbonitride (SiCN) amorphous powder together with 5% yttria as additive to the crystalline β-$Si_3N_4$ powder. The powder mixture was attrition milled in isopropanol for 4 h. The dried starting mixture was sieved through a 25 μm sieve to eliminate large agglomerates. The mixture was cold-pressed in a steel die at a pressure of 100 MPa, then embedded into a boron nitride (BN) powder bed and hot-pressed at 30 MPa and 1750°C under a 2kPa overpressure of nitrogen. The density of the hot-pressed discs (50 mm diameter) was measured by mercury immersion and exceeded 98% of the theoretical density (TD). The calculated TD was $3.26 \times 10^3$ kg/m$^3$. A reference monolithic ceramic was also prepared to study the influence of SiC particles on crack initiation and propagation during low-cyclic loading at 1350°C. Apart from addition of the amorphous SiCN, all processing steps, as well as the sintering additive, were the same as for the composite material.

Microstructure of the tested materials was studied by scanning electron microscopy (SEM) on polished and plasma etched samples and by transmission electron microscopy (TEM) and high resolution electron microscopy (HREM) on foils prepared by ion-beam thinning. The size distribution of the inter- and intragranularly located SiC nanoparticles has been evaluated using statistical analysis.

Bend test specimens with the tensile surface finish of 15 μm with dimensions of 3 x 4 x 45 mm were cut from the hot pressed discs.

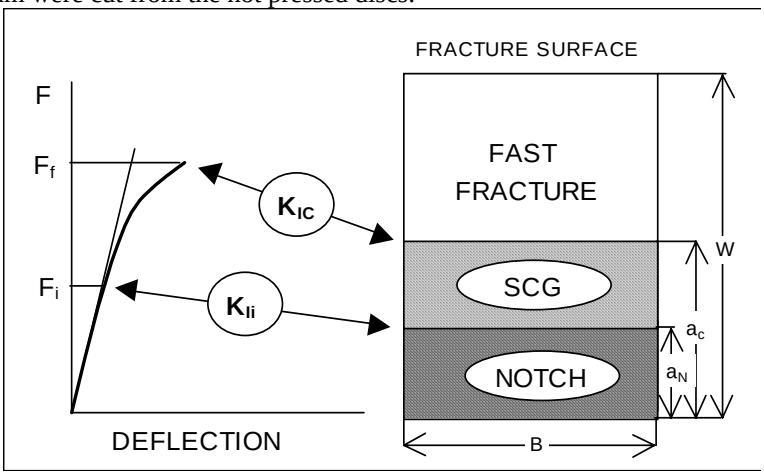


Fig.1. Schematic illustration of the experimental procedure. $K_{Ii}$ – stress intensity factor for crack initiation, $K_{IC}$-critical value of the stress intensity factor, $a_N$-depth of the sharp notch, $a_c$- critical crack size at fast fracture.

In the fracture toughness test, the sharp notch was introduced according to the VAMAS TWA#3/ESIS TC6 Round Robin Instruction [19], Fig.1. In all cases the notch tip radius was less than 10 μm. The specimens were tested in 4-point flexure with spans of 40 and 20 mm at room temperature (loading rate 0.5 mm/min) and at 1350°C at loading rates 1 mm/min, 0.5 mm/min, 0.1 mm/min and 0.01 mm/min. To establish thermal equilibrium, the specimens were held for 10 min at testing temperature prior to loading. Three specimens were tested at each loading rate. The load-deflection curve was recorded up to the specimen failure. The deviation from the initial straight part in the load-deflection curve was taken as

a manifest of slow crack growth. After the mechanical test the samples were examined using a stereo microscope at magnifications from 20 to 100x to determine the average notch length and the average slow crack growth size prior to fracture. The values of $K_{IC}$ are computed using the procedure described in [19].

Dynamic fatigue tests were conducted in four-point flexure (20/40 mm) at loading rates 1 mm/min, 0.5 mm/min, 0.1 mm/min, 0.05 mm/min and 0.01 mm/min in ambient air. The strength was calculated using the procedure given in [20].

The fatigue tests were conducted in four-point flexure (20/40 mm span) at loading/unloading rates of 0.05 mm/min at 1350°C in air. Two types of specimens have been tested, W = 4 mm and W = 3 mm, respectively, with and without a sharp notch (notch tip radius ~10 μm), at applied loads from 50 N with steps of 25 N, and from 50 N with steps of 50 N, respectively. Five cycles have been performed at all applied load levels with a loading amplitude of 50 N. The deflection of the specimens has been recorded up to the specimen failure and the critical load and deflection at failure were established. Besides this, the deflection after cycling at each load level has been measured too, (Fig.2). The failure stress of the unnotched specimens was calculated using the Hollenberg formula [20, 21].

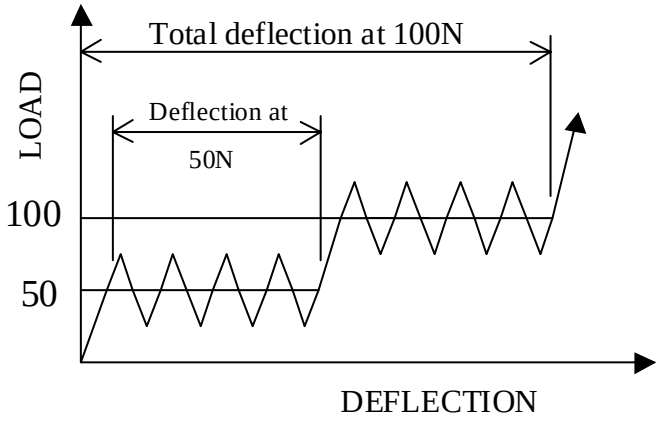


Fig.2. Schematic illustration of the low-cycle fatigue test using step loading of unnotched specimens. The test procedure for notched specimens was the same, but with increasing load steps of 25N.

According to our previous experiment [22], the nanocomposite contains processing and/or grinding flaws which cause strength degradation and degradation of the dynamic fatigue parameters. To investigate the influence of the SiC addition on the fatigue/creep performance of the $Si_3N_4$ + SiC nanocomposite the specimens where processing/grinding related defects were found as a fracture origin were not taken into consideration for the evaluation. After mechanical testing the samples were examined using a stereomicroscope at magnifications from 20x to 100x to determine the notch length and slow crack growth (SCG) size prior to fracture. Fractography was used to study the fracture micromechanisms during the slow crack growth.

The creep test in bending (20/40 inner/outer span) was performed in the temperature range from 1200°C to 1400°C, on air.

## RESULTS AND DISCUSSION

### Microstructure

Microstructure of the nanocomposite consists of $Si_3N_4$ grains with a bimodal grain-size distribution, (Fig.3a). Large grains with diameter of ~1.5-2.5 μm with a relatively low aspect ratio are observed. The intragranularly located SiC nanoparticles hamper the growth of the $Si_3N_4$ grains, and locally change their shape, (Fig.3b). The space between large $Si_3N_4$ grains is filled by $Si_3N_4$ and SiC grains, ~0.1-0.3 μm in diameter, which results in very small sized (in volume) multigrain junctions. Porosity is present in the microstructure (pores ~0.5 μm in diameter, with occasional coalescence). The relatively homogeneously distributed SiC nanoparticles are located both, intergranularly (with a size of approximately 200 nm) or intragranularly (with a size of approximately 50 nm), [11]. In agreement with the results of Pan et al. [23] HREM revealed the presence of amorphous films on the $Si_3N_4$/SiC boundaries, but also "clean" boundaries in cases where special crystallographic orientation relationships exist. The monolithic material exhibits a microstructure that is similar to that of the composite, however, with larger average grain diameter and larger multigrain junctions.

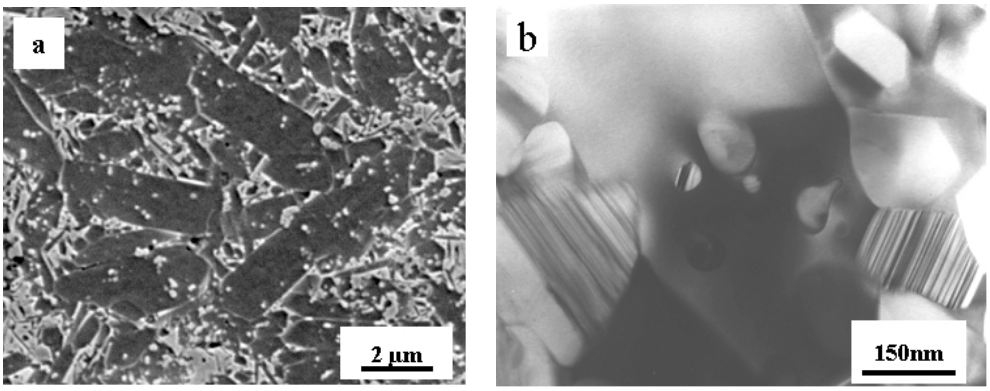


Fig.3. Characteristic microstructure of the nanocomposites a-SEM, plasma etched, b-TEM foil technigue.

### Fracture toughness

The room temperature fracture toughness of the composite and of the monolithic silicon nitride (calculated using values $a_N$, Fig.1) was 4.5 MPa $m^{0.5}$ and 5.1 $MPam^{0.5}$, respectively (standard deviation ± 0.2 $MPam^{0.5}$).

In Figure 4 the influence of the loading rate on the fracture toughness (calculated using $a_C$ values) of the both materials studied at 1350°C is illustrated. At low loading rates (below 0.1 mm/min), the fracture toughness of the composite is lower than that of the monolithic material, however, at higher loading rates the composite shows higher fracture resistance than the monolithic one.

Only at the lowest loading rate (0.01 mm/min) is it possible to determine unambiguously the load level ($F_i$) at which slow crack propagation from the notch ($a_N$) starts at 1350°C. The calculated stress intensity factor for crack initiation determined from $F_i$ and $a_N$ in monolithic and composite ceramics is 4.8 $MPam^{0.5}$ and 4.6 $MPam^{0.5}$, respectively. However, the $K_{Ii}$ values are probably load rate dependent and hence different

for different loading rates. At the highest loading rate the load-deflection curve is essentially linear, and it is possible to say that the $K_{Ii}$ is very close to $K_{IC.}$

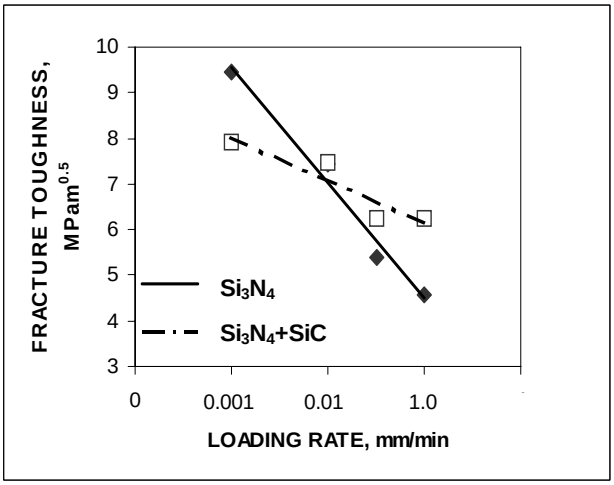


Fig.4. Effect of the loading rate on the Fracture toughness.

Slow crack growth prior to catastrophic failure has been detected at all applied loading rates at 1350$^{o}$C by fractography. The shape of the SCG area is usually symmetrical but the crack front is not a straight line. The depth of the SCG area (at the failure) is larger at the surface of the samples, which may be related to oxidation enhanced slow crack growth at this temperature. Fractographic analysis of the fracture line in the composite revealed linking of the existing micropores in the material with microvoids arising during loading.

**Dynamic fatigue strength**

Both materials show decreasing strength with decreasing loading rate, but at all loading rates (except the rate 1 mm/min where both materials show very similar strength) the mean strength of the composite is lower than that of the monolithic material, Fig.5. The SCG behaviour of the composite can be described by one number of N = 7.1 in whole interval of the applied loading rates. The SCG behaviour of the monolithic silicon nitride seems to be different; at higher loading rates it can be characterized by N = 19.8 and at low loading rates by N = 4.7.

Permanent deflection was found after failure in the monolithic material loaded at 0.01 and 0.05 mm/min. In the composite this was found only in the samples loaded at lowest loading rate and the deformation was significantly lower compared to that in monolithic material tested at the same loading rate. In monolithic and composite specimens loaded at 1 mm/min and in part of the specimens loaded at 0.5 mm/min it was not possible to identify a SCG area. In the remaining specimens a SCG area was clearly identified and in most cases it originated from the corner of the specimen. The size of this area increases with decreasing the loading rate. In the composite, the plane of the SCG area was often inclined from the plane perpendicular to the specimen axis, which indicates that the failure was initiated from an inherent flaw, probably from a surface crack. No additional cracks were identified in the specimens beside the crack causing fracture.

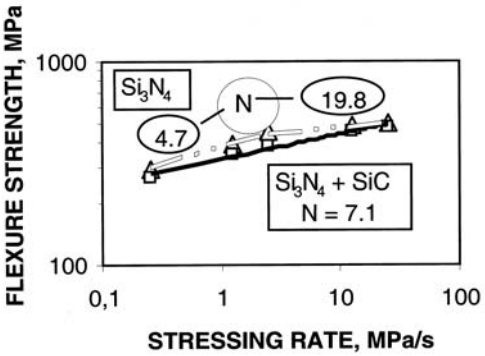


Fig.5 Effect of the stressing rate on strength.

These results are in a good agreement with the results of Wereszczak et al [7] obtained on a silicon nitride with the same additive, tested in a similar stressing interval at 1400°C ( N = 3.9).

**Low-cycle fatigue strength**

Typical load-deflection curves obtained on specimens without sharp notch are illustrated for the nanocomposite (Fig.6a) and monolithic material (Fig.6b). Their different behaviour is evident. In general, the composite exhibits higher failure load (stress) and therefore withstands higher applied loads and more cycles. The composite exhibits also less deflection at individual load levels and less total deflection at failure.

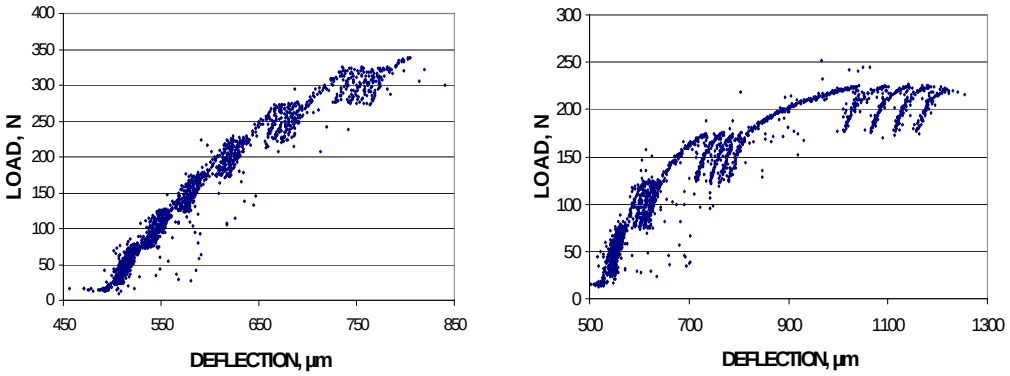


Fig 6 Load -deflection curve for a-nanocomposite and b-Si3N4.

The difference in behaviour between the monolithic material and the composite is not significant in the case of notched specimens. The deflection of monolithic silicon nitride is slightly higher at all applied loads (except at 50 N) than that for the composite, and it increases slightly faster with increasing load.

The difference in behaviour of the nanocomposite and monolithic silicon nitride is more significant for the unnotched specimens: at all applied load levels the monolithic material exhibits significantly higher “individual” and total deflections than the composite.

The current results indicate that in cyclic fatigue/creep conditions the $Si_3N_4$ + SiC nanocomposite exhibits higher deformation and fracture resistance than the monolithic

silicon nitride. The significantly different behaviour of monolithic and composite material during testing of unnotched specimens shows that the main contribution of the silicon carbide particles lies probably in the deformation and micro-crack initiation process.

**Creep behaviour**

Results of the creep experiment are summarized in Figs.7 and 8.

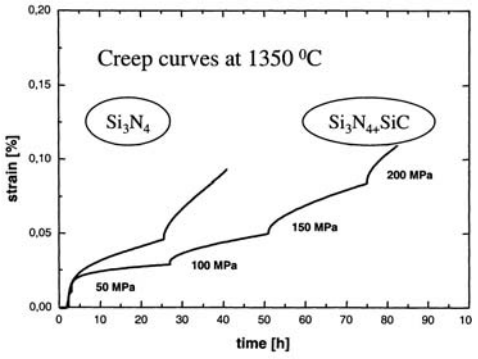


Fig 7 Creep curves at 1350°C .

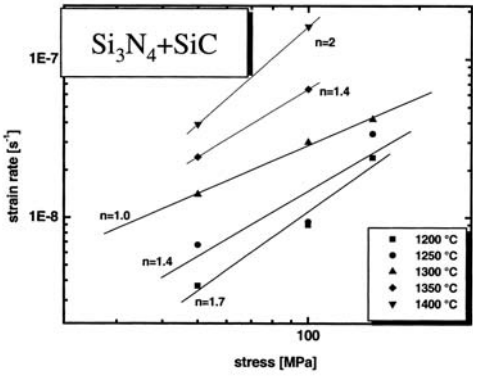


Fig 8 Creep exponents of nanocomposite.

The high temperature creep measurements show a significant improvement of creep resistance of the nanocomposite when comparing to the reference silicon nitride. The excessive carbon introduced along with SiCN amorphous powder most probably reduced the $SiO_2$ content similarly as it was observed in the model experiment, [13]. This fact has two consequences: a decreased amount of the oxide grain boundary phase, and a shift of the eutectic temperature to higher values; according to the phase diagram the next eutectic point (at a decreased content of $SiO_2$) is at 1900°C. Rendtel et al. [24] showed that there exists an optimal SiC nano-grains content which lies within the range of 10-15 wt. %. This means that a further creep resistance improvement can be achieved by optimization of the SiC content in the material.

**CONCLUSION**

A silicon nitride-silicon carbide nanocomposite was fabricated from a powder mixture of amorphous SiCN and crystalline β-$Si_3N_4$ with 5 wt% of $Y_2O_3$ additive. The influence of the addition of SiC nanoparticles on the high temperature mechanical properties have been studied in air by comparing the data obtained on the nanocomposite with those on the monolithic silicon nitride fabricated using the same processing steps as the composite.

- A rising fracture resistance was found with decreasing loading rate in both, $Si_3N_4$ + SiC composite and monolithic silicon nitride at 1350°C and it was more enhanced in the monolithic material. This can be explained by a visco-elastic deformation related energy dissipation during the slow crack growth at 1350°C, which was more pronounced in the monolithic ceramic;
- the flexure strength significantly decreases with decreasing stress rates at 1350°C in air for both ceramics, however, the strength of the composite was lower than that of the monolithic ceramics at all stress rates; stress corrosion cracking and creep damage mechanisms have been identified in the monolithic ceramics tested at low loading rates

but the mechanism responsible for specimen failure was stress corrosion cracking. Oxidation assisted slow crack growth, originating from flaws on the tensile surface (corner) of the specimens has been identified as the main strength decreasing mechanism in the composite;

- the nanocomposite exhibits higher fatigue strength than the monolithic material. This is caused by its higher resistance against the initiation and propagation of corrosion cracks as a result of the intergranularly located SiC particles which decrease the effective "cross section" of the intergranular phase and limit the oxygen transport into the bulk of the material.
- The composite exhibits significantly higher creep resistance than the monolithic silicon nitride.

**ACKNOWLEDGEMENT**

The work was carried out during J. Dusza's stay at the Institute for Advanced Materials, Joint Research Centre, Commission of the European Communities in Petten, The Netherlands and at Austrian Research Centers Seibersdorf in Seibersdorf, Austria. The work was partially supported by the Slovak Grant Agency under the contract number VEGA 2/1166/21.

**REFERENCES**

[1] Inamura, H., et al.: J. Am.Ceram.Soc., vol. 83, 2000, p. 495
[2] Sun, EY., et al.: J. Am.Ceram.Soc., vol. 81, 1998, p. 2831
[3] Cinibulk, MK., Thomas, G., Johnson, SM.: J. Am.Ceram.Soc., vol. 81, 1990, p. 1606
[4] Raj, R.: J.Am.Ceram.Soc., vol. 76, 1993, p. 2147
[5] Gogotsi, YG., Grathwohl, G.: J. Am. Ceram. Soc., vol. 76, 1993, p. 3093
[6] Dusza, J., Sajgalik, P., Steen, M.: J. Am .Ceram. Soc., vol. 82, 1999, p. 3113
[7] Wereszczak, AA., et al.: Mat. Sci. Eng. A, vol. 191, 1995, p. 257
[8] Wereszczak, AA., et al.: J.Am.Ceram.Soc., vol. 78, 1995, p. 2129
[9] Niihara, K.: J.Ceram. Soc. Jpn., vol. 99, 1991, p. 974
[10] Sternitzke, M.: J. Europ. Ceram.Soc., vol. 17, 1997, p. 1061
[11] Dusza, J., Steen, M.: Int. Mat. Rev., vol. 44, 1999, p. 165
[12] Lange, FF.: J. Am.Ceram.Soc., vol. 56, 1973, p. 445
[13] Sajgalik, P., et al.: J. Europ. Ceram. Soc., vol. 20, 2000, p. 453
[14] Niihara, K., et al.: J. Mater. Sci. Letters, vol. 9, 1999, p. 598
[15] Rendtel, A., et al.: J.Am.Ceram.Soc., vol. 81, 1998, p. 1109
[16] Besson, JL. et al.: J. Europ. Ceram. Soc., vol. 18, 1998, p. 1893
[17] Rouxel, T., Wakai, F., Sakaguchi, S.: J.Am.Ceram.Soc., vol. 77, 1994, p. 3237
[18] Herrrmann, M. et al.: Key Eng. Mat., vol. 161-163, 1999, p. 377
[19] Kübler, J.: Ceram. Eng. Sci. Proc., vol. 18, 1997, p. 155
[20] Hollemberg, GW., Terwilliger, GR., Gordon, RS.: J.Am.Ceram.Soc., vol. 54, 1971, p. 196
[21] Dusza, J., et al.: J.Mater. Sci., 2001, p. 4469
[22] Dusza, J., et al.: Mat. Sci. Eng. A, vol. 291, 2000, p. 250
[23] Pan, X., Mayer, J., Ruehle, M.: J.Amer. Ceram. Soc., vol. 79, 1996, p. 389
[24] Rendtel, A., et al.: J. Am. Ceram. Soc., vol. 81, 1998, no. 5, p. 1109